RSC Advances

PAPER

View Article Online
View Journal | View Issue

Will a graphitic-like ZnO single-layer be an ideal substrate for graphene?

Cite this: *RSC Adv.*, 2014, **4**, 17478

Qiushi Yao, Yuzhen Liu, Ruifeng Lu, Chuanyun Xiao, Kaiming Deng* and Erjun Kan*

Received 11th January 2014
Accepted 20th February 2014

DOI: 10.1039/c4ra01077a

www.rsc.org/advances

The interaction between graphene and substrates may destroy the intrinsic properties of graphene, and reduce the potential applications of graphene in electronic devices. Here, we use first-principles calculations to explore the possibility of a graphitic ZnO layer as an ideal substrate for graphene. Taking graphitic ZnO with and without oxygen vacancies, we found that the intrinsic linear dispersion of graphene is well retained. Additionally, the resultant bilayer structure of graphene and the graphitic ZnO layer shows much better optical properties compared with separate graphene and graphitic ZnO. Moreover, we also found that both the band dispersion and Fermi velocity of the bilayer structured graphene are robust towards an external electric field. Therefore, our results indicate that a graphitic ZnO layer may be a suitable substrate for graphene in real applications.

1. Introduction

Graphene, which is composed of a single layer of carbon atoms arranged in a two-dimensional (2D) honeycomb lattice, has attracted great research interest. Because of its unique properties,[1–3] graphene has been proposed as a potential material for next-generation devices, including high-speed electronic[4] and optical devices,[5] energy generation and storage,[5–7] hybrid materials,[8,9] chemical sensors,[3,10] and so on. However, in practical applications of graphene, the typical substrates, such as SiO_2,[11–13] SiC,[14–18] and some metal surfaces,[19–22] form strong interactions with graphene, which destroy the intrinsic electronic states of graphene and significantly lower its carrier mobility. So it is quite interesting to find a suitable substrate which can better preserve the intrinsic properties of graphene.

Recently, there has been more and more work focusing on the heterostructures of graphene and other 2D crystals, such as graphene/graphitic born nitride,[23–25] graphene/MoS_2 nanosheets,[26–28] graphene/$MoSe_2$ nanosheets,[29,30] graphene/graphitic carbon nitride,[31,32] and graphitic ZnO (g-ZnO).[33] Differing from traditional substrates consisting of thin films, such 2D crystal based heterostructures have shown many novel properties. Interestingly, most of these 2D crystals can preserve the high carrier mobility of graphene, and improve its optical properties.[33] Consequently, such heterostructures hold great promise for future applications.

On the other hand, almost all of the studies focus on the perfect structures of 2D crystals, and the effects of defects are totally ignored. However, in any real application, defects cannot be fully avoided. For example, when the number of layers of ZnO (0001) film is reduced, it indeed prefers a graphitic honeycomb structure.[34] However, oxygen vacancies (V_O) are naturally abundant defects in ZnO. Therefore, the prepared graphitic ZnO (g-ZnO) may contain many oxygen vacancies. For the graphene/g-ZnO bilayer structure (GZO), how oxygen vacancies affect the electronic structure of graphene is still not clear. Since oxygen vacancies bring external carriers, it is natural to ask whether g-ZnO with oxygen vacancies (g-ZnOV) could destroy the high carrier mobility of graphene.

In the present work, we investigated the electronic structure and optical properties of GZO with and without oxygen vacancies *via* first-principles calculations. Our results indicate that graphene shows weak interactions with g-ZnO and g-ZnOV. Importantly, GZO with and without oxygen vacancies can better preserve graphene's intrinsic electronic properties, high carrier mobility, and optical absorptions. Furthermore, the band dispersion and Fermi velocity of these hybrid structures are robust under an external electric field. According to our studies, g-ZnO may be a suitable substrate for graphene for practical applications in electronic and photoactive devices.

2. Computational method

Our first-principles calculations were based on density functional theory (DFT) with a generalized gradient approximation (GGA)[35] for the exchange correlation potential. The Perdew–Burke–Ernzerholf (PBE) functional was used for the GGA as implemented in the Vienna *ab initio* simulation package (VASP).[36] A van der Waals (vdW) correction proposed by Grimme (DFT-D2)[37] was chosen due to its good description of long-range vdW interactions.[38,39] The structures were relaxed without any symmetry constraints with a cutoff energy of 500 eV. Reciprocal space was represented by a Monkhorst–Pack special *k*-point

Department of Applied Physics, Nanjing University of Science and Technology, Nanjing, 210094, China. E-mail: kmdeng@njust.edu.cn; ekan@njust.edu.cn

scheme[40] with 5 × 5 × 1 grid meshes. The convergence criteria of energy and force were set to 1 × 10^{-5} eV and 0.01 eV $Å^{-1}$, respectively. A vacuum space consisting of a 17 Å normal to graphene plane was used to avoid interactions between two layers. The accuracy of our procedure was tested by calculating the C–C bond length of graphene; our calculated result of 1.407 Å is in good agreement with the experimental value of 1.420 Å.

The calculated unit cell lattice parameters for graphene and the g-ZnO monolayer were 2.46 and 3.25 Å, which fully agrees with previous experimental measurements and theoretical studies.[41,42] We constructed a supercell consisting of 32 carbon atoms, 9 oxygen atoms and 9 zinc atoms as shown in Fig. 1(a). A 4 × 4 supercell of graphene was used to match a 3 × 3 supercell of the g-ZnO monolayer. The g-ZnO monolayer was assumed to be a substrate and we used a lattice constant similar to that of g-ZnO. The lattice mismatch was only 0.92%, which was almost the most suitable supercell. For GZOs with an oxygen vacancy (GZOV), we used the term GZOV-n (n = 1, 2, 3, 4, 5, 6) to denote composite structures with different V_O positions, as shown in Fig. 1.

3. Results and discussion

As shown in Fig. 1(a), there are six possible positions for the oxygen vacancy to be located according to symmetry arguments. To find the most energetically favorable structure, we freely relaxed all of the atoms without any restriction. By calculating the total energy of different configurations (as shown in Fig. 1(b)), we found that GZOV-2 is the most stable structure, while all the other structures are higher in energy by at least 25 meV. Therefore, the following discussions are mainly focused on the GZOV-2 structure.

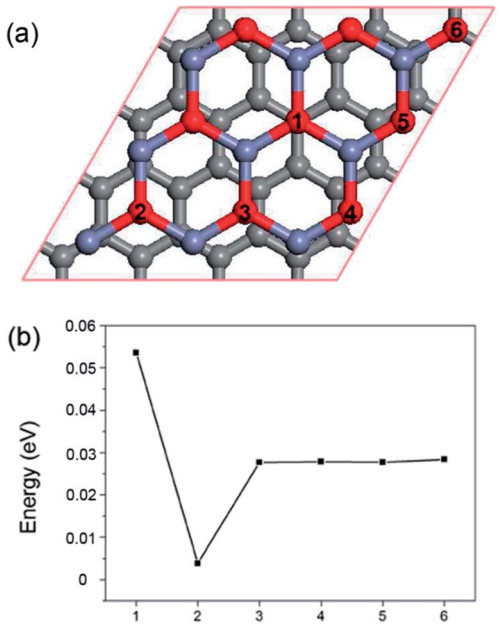

Fig. 1 (a) Optimized structure of the GZO nanocomposite. The numbers 1–6 represent six possible positions for the oxygen vacancy, which are denoted as GZOV-n (n = 1–6). The gray, red, and blue balls denote carbon, oxygen, and zinc atoms, respectively. (b) Optimized energies correspond to different composite structures. The horizontal axis 1–6, represents GZOV-1 to GZOV-6.

First of all, the electronic properties of GZO and GZOV-2 were carefully investigated. It has been well documented that monolayered graphene shows a linear dispersion relationship $E(k) = \pm\hbar v_F|k|$ (v_F is the Fermi velocity) at around the Fermi level. For the GZO system, the linear dispersion character of graphene is well preserved, as shown in Fig. 2(a). The calculated v_F of GZO is 4.89 × 10^5 m s^{-1}, which agrees well with previous studies.[33] On the other hand, for GZOV-2, it is quite surprising that the intrinsic linear dispersion of graphene is also well preserved (as shown in Fig. 2(b)), and the calculated v_F of GZOV-2 is 4.82 × 10^5 m s^{-1}, which is very close to that of free-standing graphene. Differing from hexagonal boron nitride (h-BN), both g-ZnO and g-ZnOV cannot widen the energy gap of graphene. By carefully looking at the calculated band structures of GZO and GZOV-2, we found that there were two important characteristics: (1) there was no chemical interaction between graphene and g-ZnO (g-ZnOV); and (2) the electronic states contributed by g-ZnO (g-ZnOV) were well separated with that of graphene.

To explore how the substrates affect the electronic properties of graphene, we plot differential charge densities ($\Delta\rho$ = ρ(GZO) − ρ(graphene) − ρ(g-ZnO)/ρ(g-ZnOV)) in Fig. 3. It should be noted that there is no charge transfer between graphene and substrates, because the electronic structure of graphene is well preserved. However, the inhomogeneous substrates indeed induce charge redistribution in the graphene plane, forming intralayer electron–hole puddles.[43] Now, we can understand why the GZOV-2 structure is the most favored in energy. For g-ZnOV, most of the defective states are distributed around the oxygen vacancy. Thus, the relative stability of GZOV is dominated by the coulomb interaction between the defective states of g-ZnOV and the delocalized π states. Consequently, when the oxygen vacancy is located exactly in the middle of the hexagon of graphene, the coulomb interaction is the weakest, favoring the GZOV-2.

Since GZO has shown excellent optical properties, it is interesting to study the optical properties of GZOV-2. As shown in Fig. 4, we plot the imaginary part of the dielectric functions.

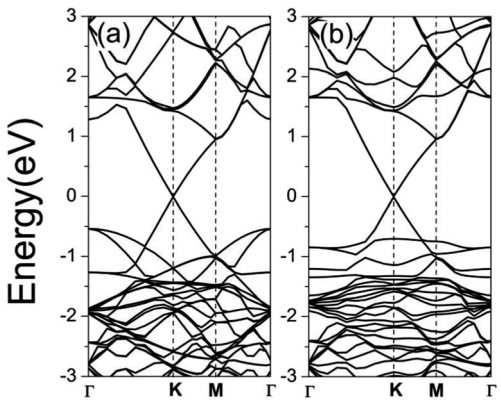

Fig. 2 Electronic band structures of (a) GZO, and (b) GZOV.

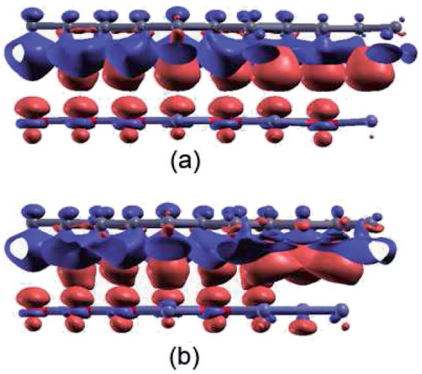

Fig. 3 Differential charge density with an isosurface value of 0.002 e $Å^{-3}$ for (a) GZO, and (b) GZOV. The red and blue regions indicate an increase and decrease in electron density, respectively.

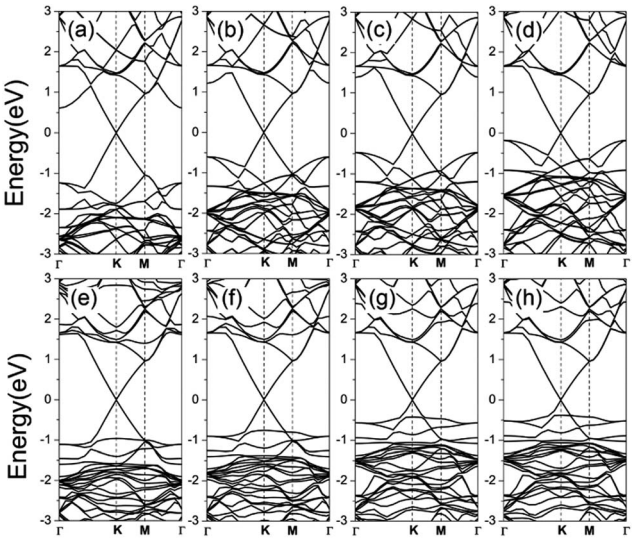

Fig. 5 Electronic band structures of (a) GZO, $E_{ext} = -3$ V nm^{-1}, (b) GZO, $E_{ext} = -1$ V nm^{-1}, (c) GZO, $E_{ext} = 1$ V nm^{-1}, (d) GZO, $E_{ext} = 3$ V nm^{-1}, (e) GZOV-2, $E_{ext} = -3$ V nm^{-1}, (f) GZOV-2, $E_{ext} = -1$ V nm^{-1}, (g) GZOV-2, $E_{ext} = 1$ V nm^{-1}, and (h) GZOV-2, $E_{ext} = 3$ V nm^{-1}. The positive direction of E_{ext} is from the g-ZnO plane to the graphene plane.

Although the absorption edges should have a rigid shift (of about 1.5 eV) due to the underestimation of the band gap in DFT calculations,[44] it has been shown that the tendency of the calculated optical properties is reasonable.[45–47] Compared with GZO, GZOV-2 exhibits similar a visible light response. More importantly, all of the other GZOV structures have similar optical properties. In other words, the positions of the oxygen vacancies do not change the optical adsorption. Therefore, g-ZnO can be used as an important substrate to enhance the optical properties of graphene, which may hold great potential in photocatalytic and photovoltaic applications.

Although we have shown that g-ZnO may be one of the most suitable substrates for graphene, it is not clear whether such a situation will be changed in real applications. As we know, an external electric field E_{ext} is inevitable for practical applications in electronic devices. Therefore, it is quite interesting to explore the response of GZO and GZOV under an external electric field. To simulate the external electric field, a sawtooth like potential was applied along the direction perpendicular to the graphene plane, and the positive direction of the electric field was defined from the g-ZnO plane to the graphene plane. Fig. 5 shows the calculated band structures of GZO and GZOV-2 under an external electric field. It is quite clear that the linear dispersion relationship around the Dirac point is robust against an external electric field. For GZO, the occupied bands resulting from g-ZnO are quickly shifted in energy by the external electric field, and are almost degenerate with the Fermi level of graphene under an external electric field of 3 V nm^{-1}. However, for GZOV-2, we can see that the relative shift in energy is much smaller than that for GZO.

On the other hand, the mobility of the carriers is the most important characteristic of graphene, and is closely related to its potential applications. From electronic band calculations, we calculated the Fermi velocities of GZO and GZOV-2 under the applied external electric field. As shown in Fig. 6 the calculated v_F of GZO decreased slightly when the field changed from −3 to

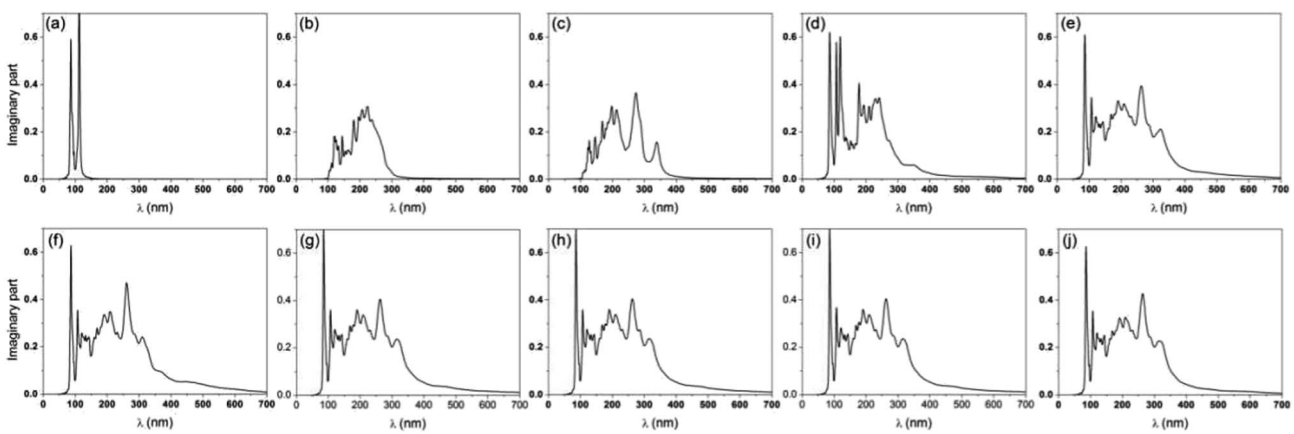

Fig. 4 Imaginary part of the dielectric function of (a) graphene, (b) g-ZnO (c) g-ZnOV, (d) GZO, (e) GZOV-1, (f) GZOV-2, (g) GZOV-3, (h) GZOV-4, (i) GZOV-5, and (j) GZOV-6 for the polarization vector perpendicular to the surface.

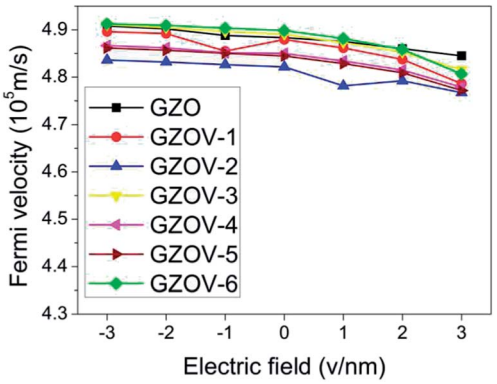

Fig. 6 Variation of the Fermi velocities of GZO and GZOV-1 to GZOV-6 against external electric field.

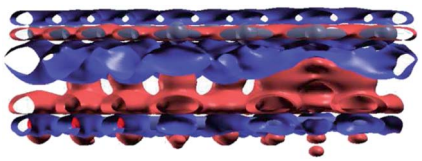

Fig. 7 Differential charge density with an isosurface value of 0.002 e Å^{-3} for GZOV-2, $E_{ext} = -3$ V nm^{-1}. The positive direction of E_{ext} is from the g-ZnO plane to the graphene plane. The red and blue regions indicate an increase and decrease in electron density, respectively.

3 V nm^{-1}, namely, ν_F changed from 4.91 $\times$ 10^5 m s^{-1} to 4.84 $\times$ 10^5 m s^{-1} with a small fluctuation of about 1.44%, which could be regarded as a constant. For GZOV-2, our calculated results showed that ν_F had the same tendency, and kept its high-speed character. For comparison, we also calculated the ν_F of all of the other GZOV structures, and found that ν_F was only changed by 2.27%, 1.95%, 1.83%, 1.87%, 2.18% for GZOV-1, GZOV-3, GZOV-4, GZOV-5, and GZOV-6, respectively. Obviously, ν_F in all of the GZOV structures gives rise to the high-speed character.

Why doesn't E_{ext} destroy the high carrier mobility of graphene? To explore this issue, we plotted the differential charge density of GZOV-2, $E_{ext} = -3$ V nm^{-1}, in Fig. 7. It is worth noting that E_{ext} does not lead to charge transfer between graphene and substrate, but induces dipole–dipole interactions to screen the external electric potential. So we come to the conclusion that the monolayered g-ZnO may be one of the most suitable substrates for graphene to preserve its intrinsic electronic properties, high carrier mobility under a wide range of external electric field regardless of oxygen vacancies, and positions of the vacancies.

4. Conclusions

In conclusion, we have theoretically demonstrated that a g-ZnO monolayer is a perfect substrate for graphene. Oxygen vacancies in g-ZnO do not have many unfavorable influences on the intrinsic electronic states of graphene, regardless of the positions of the vacancies. High carrier mobility can be preserved in both GZO and GZOV structures. Optically, oxygen vacancies do not destroy the enhanced visible light response of GZO more than simple graphene and g-ZnO monolayers. Furthermore, the band structures and Fermi velocities of GZO and GZOV are robust towards the external electric field for a wide range of field strengths.

Acknowledgements

This work was supported by the National Science Foundation of China (21203096, 11204137, 11247216, 11374160), the Natural Science Foundation of Jiangsu Province (BK20130031, BK2012392), the Fundamental Research Funds for the Central Universities (no. 30920130111016), New Century Excellent Talents in University (NCET-12-0628), Qinglan Project of Jiangsu Province, and NUST Research Funding (AB41374).

References

1 K. S. Novoselov, A. K. Geim, S. V. Morozov, D. Jiang, Y. Zhang, S. V. Dubonos, I. V. Grigorieva and A. A. Firsov, *Science*, 2004, **306**, 666–669.
2 K. S. Novoselov, A. K. Geim, S. V. Morozov, D. Jiang, M. I. Katsnelson, I. V. Grigorieva, S. V. Dubonos and A. A. Firsov, *Nature*, 2005, **438**, 197–200.
3 A. K. Geim and K. S. Novoselov, *Nat. Mater.*, 2007, **6**, 183–191.
4 Y. M. Lin, C. Dimitrakopoulos, K. A. Jenkins, D. B. Farmer, H. Y. Chiu, A. Grill and P. Avouris, *Science*, 2010, **327**, 662.
5 M. Liu, X. Yin, E. Ulin-Avila, B. Geng, T. Zentgraf, L. Ju, F. Wang and X. Zhang, *Nature*, 2011, **474**, 64–67.
6 Y. Zhu, S. Murali, M. D. Stoller, K. J. Ganesh, W. Cai, P. J. Ferreira, A. Pirkle, R. M. Wallace, K. A. Cychosz, M. Thommes, D. Su, E. A. Stach and R. S. Ruoff, *Science*, 2011, **332**, 1537–1541.
7 K. S. Kim, Y. Zhao, H. Jang, S. Y. Lee, J. M. Kim, K. S. Kim, J. H. Ahn, P. Kim, J. Y. Choi and B. H. Hong, *Nature*, 2009, **457**, 706–710.
8 M. F. El-Kady, V. Strong, S. Dubin and R. B. Kaner, *Science*, 2012, **335**, 1326–1330.
9 X. Yang, M. Xu, W. Qiu, X. Chen, M. Deng, J. Zhang, H. Iwai, E. Watanabe and H. Chen, *J. Mater. Chem.*, 2011, **21**, 8096–8103.
10 M. Deng, X. Yang, M. Silke, W. M. Qiu, M. S. Xu, G. Borghs and H. Z. Chen, *Sens. Actuators, B*, 2011, **158**, 176–184.
11 M. Ishigami, J. H. Chen, W. G. Cullen, M. S. Fuhrer and E. D. Williams, *Nano Lett.*, 2007, **7**, 1643–1648.
12 P. Shemella and S. K. Nayak, *Appl. Phys. Lett.*, 2009, **94**, 032101.
13 T. C. Nguyen, M. Otani and S. Okada, *Phys. Rev. Lett.*, 2011, **106**, 106801.
14 S. Y. Zhou, G. H. Gweon, A. V. Fedorov, P. N. First, W. A. de Heer, D. H. Lee, F. Guinea, A. H. Castro Neto and A. Lanzara, *Nat. Mater.*, 2007, **6**, 770–775.
15 A. Mattausch and O. Pankratov, *Phys. Rev. Lett.*, 2007, **99**, 076802.
16 F. Varchon, R. Feng, J. Hass, X. Li, B. N. Nguyen, C. Naud, P. Mallet, J. Y. Veuillen, C. Berger, E. H. Conrad and L. Magaud, *Phys. Rev. Lett.*, 2007, **99**, 126805.

17 S. Kim, J. Ihm, H. J. Choi and Y. W. Son, *Phys. Rev. Lett.*, 2008, **100**, 176802.
18 J. Ristein, S. Mammadov and T. Seyller, *Phys. Rev. Lett.*, 2012, **108**, 246104.
19 G. Giovannetti, P. A. Khomyakov, G. Brocks, V. M. Karpan, J. van den Brink and P. J. Kelly, *Phys. Rev. Lett.*, 2008, **101**, 026803.
20 P. A. Khomyakov, G. Giovannetti, P. C. Rusu, G. Brocks, J. van den Brink and P. J. Kelly, *Phys. Rev. B: Condens. Matter Mater. Phys.*, 2009, **79**, 195425.
21 C. Gong, G. Lee, B. Shan, E. M. Vogel, R. M. Wallace and K. Cho, *J. Appl. Phys.*, 2010, **108**, 123711.
22 M. Vanin, J. J. Mortensen, A. K. Kelkkanen, J. M. Garcia-Lastra, K. S. Thygesen and K. W. Jacobsen, *Phys. Rev. B: Condens. Matter Mater. Phys.*, 2010, **81**, 081408.
23 G. Giovannetti, P. A. Khomyakov, G. Brocks, P. J. Kelly and J. van den Brink, *Phys. Rev. B: Condens. Matter Mater. Phys.*, 2007, **76**, 073103.
24 C. R. Dean, A. F. Young, I. Meric, C. Lee, L. Wang, S. Sorgenfrei, K. Watanabe, T. Taniguchi, P. Kim, K. L. Shepard and J. Hone, *Nat. Nanotechnol.*, 2010, **5**, 722–726.
25 Y. C. Fan, M. W. Zhao, Z. H. Wang, X. J. Zhang and H. Y. Zhang, *Appl. Phys. Lett.*, 2011, **98**, 083103–083103.
26 K. Chang and W. Chen, *Chem. Commun.*, 2011, **47**, 4252–4254.
27 Y. Ma, Y. Dai, M. Guo, C. Niu and B. Huang, *Nanoscale*, 2011, **3**, 3883–3887.
28 L. Britnell, R. V. Gorbachev, R. Jalil, B. D. Belle, F. Schedin, A. Mishchenko, T. Georgiou, M. I. Katsnelson, L. Eaves, S. V. Morozov, N. M. R. Peres, J. Leist, A. K. Geim, K. S. Novoselov and L. A. Ponomarenko, *Science*, 2012, **335**, 947–950.
29 J. N. Coleman, M. Lotya, A. O'Neill, S. D. Bergin, P. J. King, U. Khan, K. Young, A. Gaucher, S. De, R. J. Smith, I. V. Shvets, S. K. Arora, G. Stanton, H.-Y. Kim, K. Lee, G. T. Kim, G. S. Duesberg, T. Hallam, J. J. Boland, J. J. Wang, J. F. Donegan, J. C. Grunlan, G. Moriarty, A. Shmeliov, R. J. Nicholls, J. M. Perkins, E. M. Grieveson, K. Theuwissen, D. W. McComb, P. D. Nellist and V. Nicolosi, *Science*, 2011, **331**, 568–571.
30 Y. Ma, Y. Dai, W. Wei, C. Niu, L. Yu and B. Huang, *J. Phys. Chem. C*, 2011, **115**, 20237–20241.
31 Q. Xiang, J. Yu and M. Jaroniec, *J. Phys. Chem. C*, 2011, **115**, 7355–7363.
32 A. Du, S. Sanvito, Z. Li, D. Wang, Y. Jiao, T. Liao, Q. Sun, Y. H. Ng, Z. Zhu, R. Amal and S. C. Smith, *J. Am. Chem. Soc.*, 2012, **134**, 4393–4397.
33 W. Hu, Z. Li and J. Yang, *J. Chem. Phys.*, 2013, **138**, 124706.
34 C. Tusche, H. L. Meyerheim and J. Kirschner, *Phys. Rev. Lett.*, 2007, **99**, 026102.
35 J. P. Perdew, K. Burke and M. Ernzerhof, *Phys. Rev. Lett.*, 1996, **77**, 3865–3868.
36 G. Kresse and J. Furthmüller, *Phys. Rev. B: Condens. Matter Mater. Phys.*, 1996, **54**, 11169–11186.
37 S. Grimme, *J. Comput. Chem.*, 2006, **27**, 1787–1799.
38 S. Grimme, C. Mück-Lichtenfeld and J. Antony, *J. Phys. Chem. C*, 2007, **111**, 11199–11207.
39 V. Caciuc, N. Atodiresei, M. Callsen, P. Lazić and S. Blüge, *J. Phys.: Condens. Matter*, 2012, **24**, 424214.
40 H. J. Monkhorst and J. D. Pack, *Phys. Rev. B: Solid State*, 1976, **13**, 5188–5192.
41 A. H. Castro Neto, F. Guinea, N. M. R. Peres, K. S. Novoselov and A. K. Geim, *Rev. Mod. Phys.*, 2009, **81**, 109–162.
42 H. Y. Guo, Y. Zhao, N. Lu, E. J. Kan, X. C. Zeng, X. J. Wu and J. L. Yang, *J. Phys. Chem. C*, 2012, **116**, 11336–11342.
43 J. Martin, N. Akerman, G. Ulbricht, T. Lohmann, J. Smet, K. Von Klitzing and A. Yacoby, *Nat. Phys.*, 2007, **4**, 144–148.
44 S. Lany and A. Zunger, *Phys. Rev. B: Condens. Matter Mater. Phys.*, 2008, **78**, 235104.
45 A. Du, Y. H. Ng, N. J. Bell, Z. Zhu, R. Amal and S. C. Smith, *J. Phys. Chem. Lett.*, 2011, **2**, 894–899.
46 F. Wu, Y. Liu, G. Yu, D. Shen, Y. Wang and E. Kan, *J. Phys. Chem. Lett.*, 2012, **3**, 3330–3334.
47 J.-H. Yang, Y. Zhai, H. Liu, H. Xiang, X. Gong and S.-H. Wei, *J. Am. Chem. Soc.*, 2012, **134**, 12653–12657.

